# Extended formulation of stress concentration factors for concrete-filled steel tubular (CFST) T-joints

Jian Zheng [1]; Shozo Nakamura [2]; Yajing Ge [3]; Kangming Chen [4]; and Qingxiong Wu [5]

[1] Ph.D., Dept. of Civil and Environmental Eng., Nagasaki University, 1-14, Bunkyo-machi, Nagasaki 852-8521, Japan.

[2] Professor, Dept. of Civil and Environmental Eng., Nagasaki University, 1-14, Bunkyo-machi, Nagasaki 852-8521, Japan (corresponding author). E-mail address: shozo@nagasaki-u.ac.jp

[3] Engineer, Hokuriku Branch, Nippon Engineering Consultants Co.,Ltd., 633 Gankaiji, Toyama 930-0175, Japan.

[4] Associate professor, College of Civil Eng., Fuzhou University, No. 2, Xueyuan Road, Fuzhou 350116, China.

[5] Professor, College of Civil Eng., Fuzhou University, No. 2, Xueyuan Road, Fuzhou 350116, China.

## Abstract

In previous research, the authors numerically investigated 212 finite element (FE) models of concrete-filled steel tubular (CFST) T-joints under axial force in the brace to derive formulae for stress concentration factors (SCFs). The formulations involve four non-dimensional parameters: diameter ratio, $\beta$; diameter to thickness ratio of chord, $2\gamma$; thickness ratio, $\tau$; and relative chord length, $\alpha$. In the current study, the earlier formulation is extended to include four additional loading conditions: in-plane bending (IPB) in the brace, out-of-plane bending (OPB) in the brace, axial compression in the chord, and IPB in the chord. The validity of the new SCF formulae is demonstrated by comparing the SCFs obtained using the formulae with the results of numerical analysis.

**Keywords:** CFST T-joints; Stress concentration factors; Hot spot stress; Fatigue; Finite element analysis; Parametric formulae.

## Introduction

The trussed arch rib system is commonly used for concrete-filled steel tubular (CFST) arch bridges in China, accounting for approximately 38% of all CFST arch bridges (Wang et al. 2016a). Joints in the CFST structure are considered weak points, since the axial stiffness of the brace is much greater than the radial stiffness of the chord tube, leading to a high stress concentration at the joint. In fact, fatigue damage to CFST joints has been observed in existing bridges (Wang et al. 2016b). However, there has been very limited effort to develop formulae for stress concentration factors (SCFs) for CFST joints. The Chinese code JTG/T D65-06-2015 (Ministry of Transport of China 2015) only specifies an allowable value of nominal stress amplitude for the fatigue checking of CFST joints. On the other hand, it is generally accepted that the fatigue life of tubular joints can be estimated from SCFs using the hot-spot stress (HSS) method. The development of a series of parametric formulae for calculating SCFs has been awaited to simplify HSS calculations for CFST joints.

In previous research (Zheng et al. 2018), three-dimensional finite element (FE) models of CFST T-joints with the brace in axial tension were developed in order to replicate the results of published experiments (Chen et al. 2010; Chen 2011; Wang et al. 2011; Xu et al. 2015). After confirming the precision of these FE models, they were employed for parametric analysis to reveal the influences of certain non-dimensional parameters. Finally, parametric SCF formulae for this loading condition were developed and their accuracy was verified. The resulting formulae take into account the influences of four parameters: diameter ratio $\beta$ (= $d/D$), diameter to thickness ratio of the chord $2\gamma$ (= $D/T$), thickness ratio $\tau$ (= $t/T$) and relative chord length $\alpha$ (= $2L/D$) (see Fig. 1).

Although any bending moment in the brace is generally small and the SCFs associated with forces in the chord are minor, parametric SCF formulae for these loading conditions, which can be treated as supplementary in the overall fatigue design of CFST T-joints, are also necessary for accurate evaluations. In the current research, the applicability of the FE modelling used in the previous research to in-plane bending (IPB) in the brace is first validated. Numerical results from FE models incorporating IPB are compared with previously reported experimental results (Chen et al. 2010; Chen 2011; Wang et al. 2011; Xu et al. 2015). The validated models are then used for parametric analysis under four loading conditions: IPB in the brace, out-of-plane bending (OPB) in the brace, axial compression in the chord and IPB in the chord. Using the results of this parametric analysis, SCF formulae for CFST T-joints under these four loading conditions are proposed as functions of the non-dimensional parameters. Finally, the accuracy of the developed formulae is evaluated under each loading condition by comparing with the FE results.

## Parametric analysis

### *Description of the analysis*

The general-purpose FE analysis software MSC.Marc was used in the numerical investigation. Linear elastic analysis in terms of material properties was applied. The settings used in the FE models for material properties, element types, mesh specifications and the generation process, and the modeling of the interface between chord tube and concrete are the same as in the authors' earlier research (Zheng et al. 2018). The method of determining HSS is also the same. The chord is simply supported and chord torsion is fixed in all FE models. One of the FE models is shown in Fig. 2 with the boundary conditions.

The SCF formulae for circular hollow-section T-joints (Zhao et al. 2000) and published experimental results (Chen et al. 2010; Chen 2011; Wang et al. 2011; Xu et al. 2015) indicate that the parameters $\beta$, $2\gamma$ and $\tau$ are the key to determination of SCFs for CFST T-joints under IPB in the brace and under axial compression and IPB in the chord. On the other hand, parameter $\alpha$ is considered an additional key parameter when the brace is subjected to OPB. Therefore, in the models with IPB in the brace, axial compression and IPB in the chord, parameters $\beta$, $2\gamma$ and $\tau$ were changed but held parameter $\alpha$ constant ($\alpha$ = 12). Meanwhile, in the model where the brace was subjected to OPB, parameters, $\beta$, $2\gamma$, $\tau$ and $\alpha$ were all varied.

For the parametric analysis, these non-dimensional parameters were varied according to analysis of geometric parameter statistics for CFST K-joints in 119 CFST trussed arch bridges in China (Zheng et al. 2017). The resulting parameter ranges were $\beta$ = 0.3 – 0.6, $2\gamma$ = 40 – 80, $\tau$ = 0.4 – 1.0 and $\alpha$ = 8 – 16 and the actual parameter values were obtained by varying $d$, $T$, $t$ and $L$, respectively. The geometric dimensions of the standard FE model were set to $D$ = 600 mm, $d$ = 300 mm, $T$ = $t$ = 12 mm and $L$ = 3600 mm in reference to typical dimensions of CFST trussed arch bridges and are the same as in the earlier research (Zheng et al. 2018). Length $l$ of the brace was unchanged during the analysis at $3d$.

### *Loading conditions*

As already mentioned, four loading conditions that were not used in the previous research (Zheng et al. 2018) were applied: (a) IPB in the brace; (b) OPB in the brace; (c) axial compression in the chord; and (d) IPB in the chord. When subjected to IPB in the brace, the maximum SCFs always occurred at the chord crown (CC) or brace crown (BC), while the SCFs at the chord saddle (CS) and brace saddle (BS) were very small. Under OPB in the brace, the maximum SCFs always occurred at the CS or BS, while the SCFs at the CC and BC were very small. IPB and axial compression in the chord always induced the maximum SCFs at the CC, while the SCFs at the CS, BC and BS were very small. SCFs were calculated at these maximal locations. The loading conditions and their associated HSS locations are shown in Fig. 3. The values of $F_b$, $F_c$ and $M_c$ in Fig. 3 were determined by trial-and-error as 1000 N, $1\times10^6$ N, and $1\times10^8$ N·mm, respectively, to guarantee that the maximum HSSs are lower than the yield stress in all FE models. The maximum HSSs in loading condition (a), (b), (c) and (d) are 20.1 MPa, 29.5 MPa, -21.0 MPa and 24.6 MPa, respectively.

### *Definition of nominal stress*

The nominal stresses under bending moment in the brace ($M_b$), axial compression in the chord ($F_c$) and bending moment in the chord ($M_c$) were determined as $M_b/W_b$, $F_c/A$ and $M_c/W$, respectively. $M_b$ is the applied bending moment in the brace, obtained as the product of the applied load $F_b$ at the brace end and the distance from the loading point to the chord-brace intersection. $W_b$ is the section modulus of the brace. $A$ and $W$ are the area and section modulus of the equivalent steel tube section of the concrete-filled chord, respectively.

### ***Validation of FE models***

FE models were developed as described to simulate the experimental specimens described in the published research cited above (Chen et al. 2010; Chen 2011; Wang et al. 2011; Xu et al. 2015). The dimensions, boundary conditions and linear elastic material properties used in the models were determined based on the experimental specimens by applying the methods used in the authors' previous research (Zheng et al. 2018). The models were then validated numerically by applying IPB to the brace.

The SCF values at four locations (CC and BC on both tensile and compressive sides) obtained in the FE analysis ($SCF_{FEA}$) are compared with those from the published tests ($SCF_{Test}$) in Fig. 4. There is good agreement between the numerical results and the published experiments. This validates the models for the calculation of SCFs for CFST T-joints under IPB in the brace. Similar validations cannot be carried out for other loading conditions since there are no available test results with which the FE results can be compared.

## Proposed formulae and accuracy verification

### *Proposed formulae*

Using multiple regression analysis, formulae for determining SCFs in the chord and brace of CFST T-joints under different loading conditions are obtained as follows.

(1) Under IPB in the brace

Location CC

$$\begin{aligned} \mathrm{SCF_{CC}} &= 1.765\gamma^{0.268}\tau^{0.869}\beta^{-0.100} && \text{(tension)} \quad (1a) \\ &= 4.948\gamma^{-0.363}\tau^{1.036}\beta^{-0.550} && \text{(compression)} \quad (1b) \end{aligned}$$

Location BC

$$\begin{aligned} \mathrm{SCF_{BC}} &= 1.575\gamma^{0.121}\beta^{-0.289}[0.901-0.867(\tau-0.591)^2] && 40 \le 2\gamma \le 60 \quad \text{(tension)} \quad (2a) \\ &= 6.373\gamma^{-0.290}\beta^{-0.289}[0.901-0.867(\tau-0.591)^2] && 60 < 2\gamma \le 80 \quad \text{(tension)} \quad (2b) \\ &= 1.536\gamma^{0.184}\tau^{0.431}\beta^{-0.361} && \text{(compression)} \quad (2c) \end{aligned}$$

(2) Under OPB in the brace

Location CS

$$\begin{aligned} \mathrm{SCF_{CS}} &= 2.102\gamma^{0.396}\tau^{0.904}[1.145-6.927(\beta-0.434)^2] && \text{(tension)} \quad (3a) \\ &= 7.737\gamma^{-0.671}\tau^{0.914}\beta^{-0.928} && \text{(compression)} \quad (3b) \end{aligned}$$

Location BS

$$\begin{aligned} \mathrm{SCF_{BS}} &= 1.082\gamma^{0.447}\tau^{0.259}[1.141-6.761(\beta-0.451)^2] && \text{(tension)} \quad (4a) \\ &= 0.655\gamma^{0.324}\tau^{0.504}\beta^{-0.948} && \text{(compression)} \quad (4b) \end{aligned}$$

(3) Under axial compression in the chord

Location CC

$$\mathrm{SCF_{CC}} = 2.425\gamma^{-0.237}\tau^{0.135}\beta^{-0.134} \quad (5)$$

(4) Under IPB in the chord

Location CC

$$\mathrm{SCF_{CC}} = 2.927\gamma^{-0.240}\tau^{0.204}\beta^{-0.060} \quad (6)$$

The validity ranges of these proposed parametric formulae are $0.3 \le \beta \le 0.6$, $40 \le 2\gamma \le 80$ and $0.4 \le \tau \le 1.0$ since the formulae have been checked only for those ranges.

### *Accuracy verification*

SCFs obtained using the proposed formulae, $SCF_{FOR}$, were compared with those from FE analysis, $SCF_{FEA}$, for all locations so as to verify the accuracy of the formulae. The results are shown in Fig. 5. Also shown in the figure are statistical measures of the ratio $SCF_{FOR}/SCF_{FEA}$. Overall, there is good agreement between the two sets of SCFs. The mean values of $SCF_{FOR}/SCF_{FEA}$ listed in Fig. 5 are very close to 1.0 for all locations, and the corresponding coefficients of variance (COV) are relatively small. Therefore, it can be concluded that the proposed SCF formulae have sufficient accuracy and reliability for CFST T-joints under the four loading conditions analyzed.

## Conclusions

A previously developed finite element (FE) modeling method for CFST T-joints is first validated against published experimental results for a loading condition not considered in the earlier research: in-plane bending in the brace. After validation, the models are used for a parametric study under four loading conditions (in-plane and out-of-plane bending in the brace, axial compression in the chord and in-plane bending in the chord) to reveal the influence of geometric parameters on the stress concentration factors (SCFs). Based on the results, parametric SCF formulae corresponding to each loading condition are proposed, and their accuracy and reliability in calculating SCFs is demonstrated by comparison with the FE analysis results.

## Data Availability Statement

Some or all data, models, or code generated or used during the study are available from the corresponding author by request.

## Acknowledgments

This research was financially supported by the National Natural Science Foundation of China (No. 51408132) and China Scholarship Council (No. 201506650004).

## References

Chen, J. (2011). "Experimental and theoretical study of dynamic performance of concrete-filled steel tubular T-joints." Ph.D. thesis, Zhejiang Univ., Hangzhou, China. (In Chinese)

Chen, J., Chen, J. and Jin, W. L. (2010). "Experiment investigation of stress concentration factor of concrete-filled tubular T joints." *Journal of Constructional Steel Research*, 66(12), 1510–1515.

Ministry of Transport of China. (2015). "Specifications for design of highway concrete-filled steel tubular arch bridge." *JTG/T D65-06-2015*. China Communication Press, Beijing, China. (In Chinese)

Wang, K., Tong, L. W., Zhu, J., Zhao, X.L. and Mashiri, F. R. (2011). "Fatigue behavior of welded T-joints with a CHS brace and CFCHS chord under axial loading in the brace." *Journal of Bridge Engineering*, ASCE, 18(2), 142–152.

Wang, Q., Nakamura, S., Chen, K. M., Chen, B. C. and Wu, Q. X. (2016a). "Comparison between steel and concrete-filled steel tubular arch bridges in China." *Proceedings of constructional steel*, Japanese Society of Steel Construction, 24, 66–73.

Wang, Q., Nakamura, S., Chen, K. M., Chen, B. C. and Wu, Q. X. (2016b). "Fatigue evaluation of K-joint in a half-through concrete-filled steel tubular trussed arch bridge in china by hot spot stress method." *Proceedings of constructional steel*, Japanese Society of Steel Construction, 24, 633–640.

Xu, F., Chen, J. and Jin, W. L. (2015). "Experimental investigation of SCF distribution for thin-walled concrete-filled CHS joints under axial tension loading." *Thin-Walled Structures*, 93, 149–157.

Zhao, X. L., Herion, S., Packer, J. A., Puthli, R., Sedlacek, G., Wardenier, J., et al. (2000). "Design guide for circular and rectangular hollow section joints under fatigue loading." CIDECT, TUV.

Zheng, J., Nakamura, S., Chen, K. M. and Wu, Q.X. (2017). "Numerical Parameter Analysis on Stress Concentration Factors of Concrete-filled Steel Tubular (CFST) K-joint under Axial Loading." *The 2017 World Congress on Advances in Structural Engineering and Mechanics*, Seoul, Korea.

Zheng, J., Nakamura, S., Ge, Y. J., Chen, K. M. and Wu, Q. X. (2018). “Formulation of stress concentration factors for concrete-filled steel tubular (CFST) T-joints under axial force in the brace.” *Engineering Structures*, 170, 103–117.

**Figure captions**

Fig. 1. Geometric parameters of CFST T-joints. (a) Three-dimensional diagram; (b) Geometric parameters.

Fig. 2. FE model with the boundary conditions and local mesh around the intersection. (a) FE model; (b) Local mesh around the intersection.

Fig. 3. Loading conditions and their hot spot locations. (a) IPB in the brace; (b) OPB in the brace; (c) Axial compression in the chord; (d) IPB in the chord.

Fig. 4. Comparison of $SCF_{FEA}$ with $SCF_{Test}$

Fig. 5. Comparison of $SCF_{FOR}$ with $SCF_{FEA}$. (a) $SCF_{CC}$ under IPB in the brace; (b) $SCF_{BC}$ under IPB in the brace; (c) $SCF_{CS}$ under OPB in the brace; (d) $SCF_{BS}$ under OPB in the brace; (e) $SCF_{CC}$ under axial force in the chord; (f) $SCF_{CC}$ under IPB in the chord.

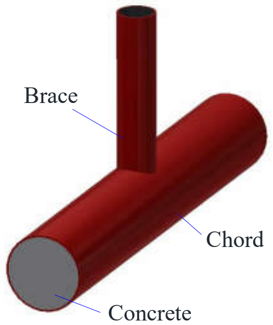

Brace
Chord
Concrete


(a)

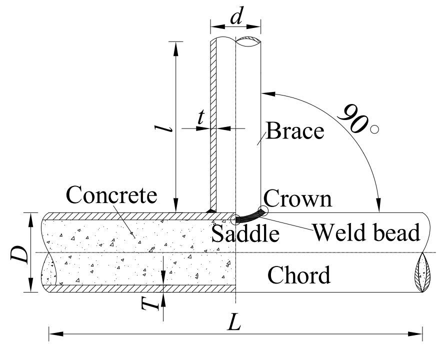

d
l
t
90°
Brace
Concrete
Crown
Saddle
Weld bead
D
Chord
T
L


(b)

Fig. 1

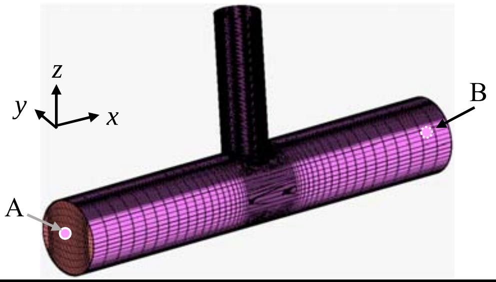


| Node | D$x$ | D$y$ | D$z$ | R$x$ | R$y$ | R$z$ |
|---|---|---|---|---|---|---|
| A | Fix | Fix | Fix | Fix | Free | Free |
| B | Free | Fix | Fix | Fix | Free | Free |

(a)

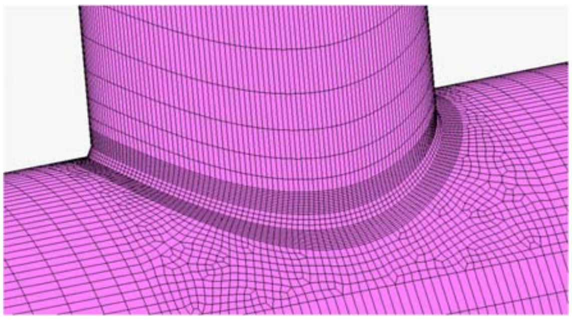

(b)

Fig. 2

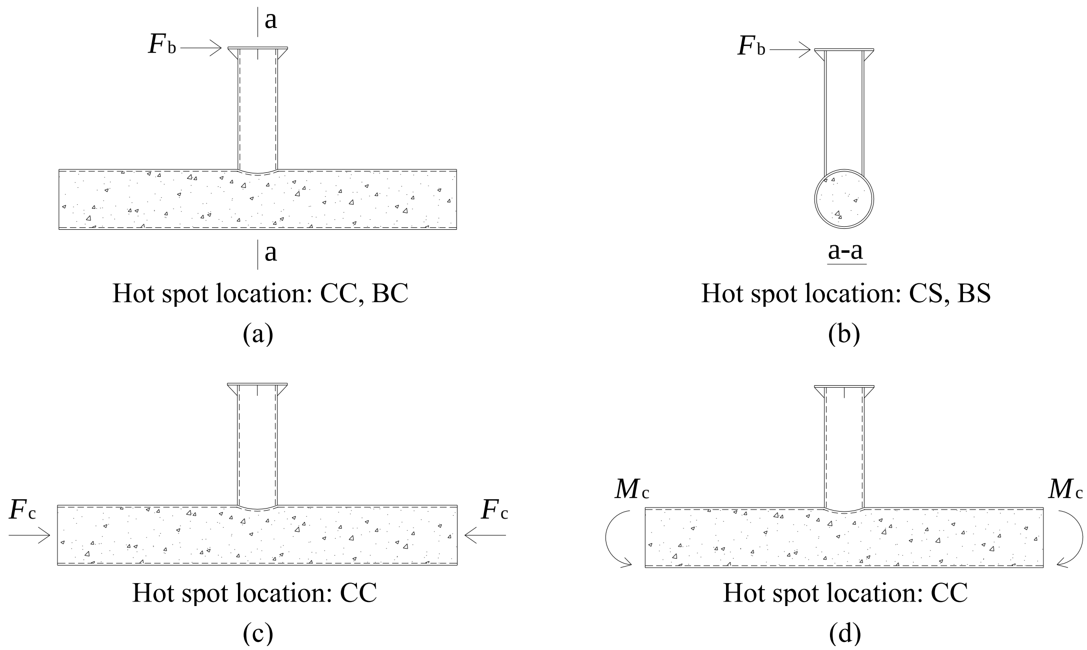

a
$F_b$
a
Hot spot location: CC, BC
(a)
$F_b$
a-a
Hot spot location: CS, BS
(b)
$F_c$
$F_c$
Hot spot location: CC
(c)
$M_c$
$M_c$
Hot spot location: CC
(d)


Fig. 3

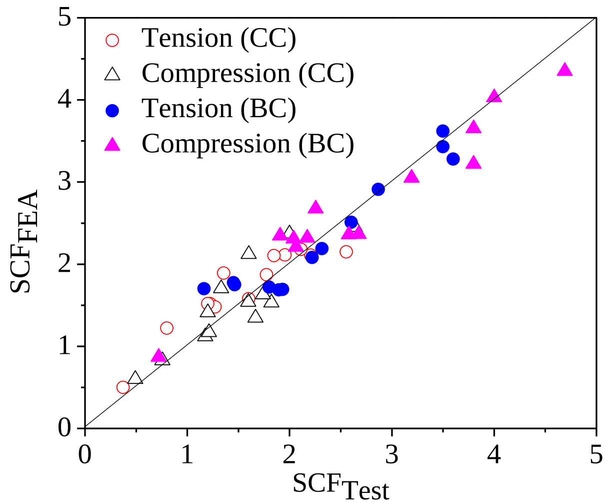

Tension (CC)
Compression (CC)
Tension (BC)
Compression (BC)
SCF_FEA
SCF_Test
0
1
2
3
4
5


Fig. 4

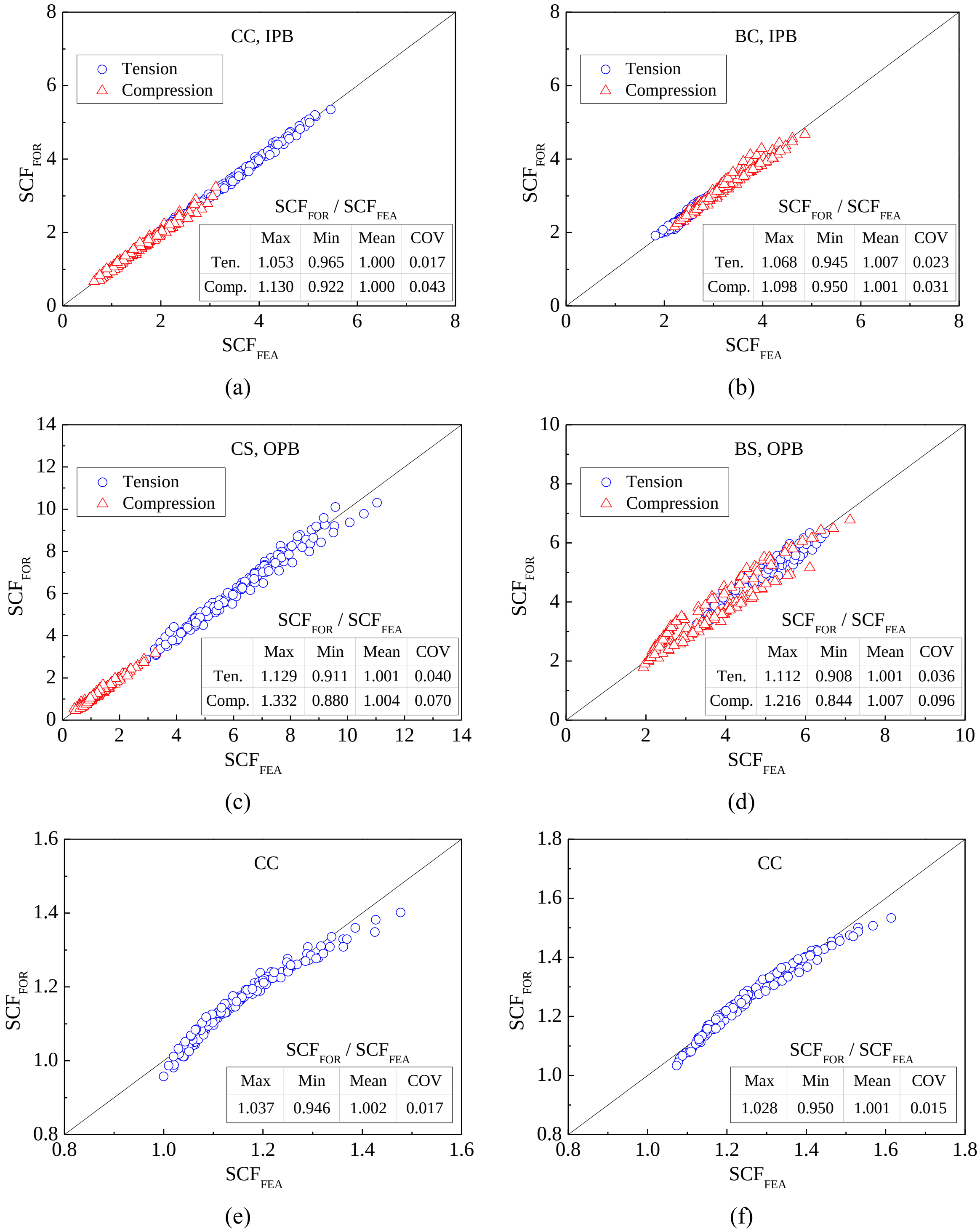
CC, IPB
Tension
Compression
SCF_FOR
SCF_FEA
SCF_FOR / SCF_FEA
Max Min Mean COV
Ten. 1.053 0.965 1.000 0.017
Comp. 1.130 0.922 1.000 0.043
(a)
BC, IPB
Tension
Compression
SCF_FOR
SCF_FEA
SCF_FOR / SCF_FEA
Max Min Mean COV
Ten. 1.068 0.945 1.007 0.023
Comp. 1.098 0.950 1.001 0.031
(b)
CS, OPB
Tension
Compression
SCF_FOR
SCF_FEA
SCF_FOR / SCF_FEA
Max Min Mean COV
Ten. 1.129 0.911 1.001 0.040
Comp. 1.332 0.880 1.004 0.070
(c)
BS, OPB
Tension
Compression
SCF_FOR
SCF_FEA
SCF_FOR / SCF_FEA
Max Min Mean COV
Ten. 1.112 0.908 1.001 0.036
Comp. 1.216 0.844 1.007 0.096
(d)
CC
SCF_FOR
SCF_FEA
SCF_FOR / SCF_FEA
Max Min Mean COV
1.037 0.946 1.002 0.017
(e)
CC
SCF_FOR
SCF_FEA
SCF_FOR / SCF_FEA
Max Min Mean COV
1.028 0.950 1.001 0.015
(f)

Fig. 5